Astron. Astrophys. 325, 943–953 (1997)

ASTRONOMY AND ASTROPHYSICS

A VLBI study of GHz-peaked-spectrum radio sources

I. VLBI images at 6 cm

C. Stanghellini[1,6], **C.P. O'Dea**[2], **S.A. Baum**[2], **D. Dallacasa**[3,5], **R. Fanti**[4,5], **and C. Fanti**[4,5]

[1] Istituto di Radioastronomia del CNR, C.P. 141, I-96017 Noto SR, Italy
[2] Space Telescope Science Institute, 3700 San Martin Drive, Baltimore, MD 21218, USA
[3] Joint Institute for VLBI in Europe, Postbus 2, 7990 AA Dwingeloo, The Netherlands
[4] Dipartimento di Fisica, Università degli Studi, via Irnerio 46, I-40126 Bologna, Italy
[5] Istituto di Radioastronomia del CNR, Via Gobetti 101, I-40129 Bologna, Italy
[6] Visitor at the Space Telescope Science Institute, Baltimore, USA

Received 10 February 1997 / Accepted 24 March 1997

Abstract. Global VLBI observations at 5 GHz of 9 powerful GHz-Peaked-Spectrum (GPS) radio sources from a complete sample of 33 objects (Stanghellini 1992, Stanghellini et al. 1996,1997) are presented. These sources have higher turnover frequencies and smaller overall sizes than Compact Steep-Spectrum (CSS) radio sources, but they are probably related objects with the apparent differences due to a different density of the ambient medium and/or a different age.

The GPS radio sources presented here show a variety of morphologies and have angular sizes ranging from a few to a hundred mas, corresponding to projected linear sizes from a few to hundreds of parsecs.

GPS quasars are rather compact and show core-jet or complex structures and may appear shortened by projection. In contrast, the GPS radio galaxies have larger sizes and exhibit a combination of jets/hot-spots/lobes on both sides of a putative center of activity. Therefore all the radio galaxies observed here can tentatively be classified as Compact Symmetric Objects (CSO). Observations at another frequency (at least) are needed to locate the core, confirm the classification and determine the spectral index of the various components.

Asymmetries in the flux densities and structures of the two opposite sides of our candidate CSO's are more likely produced by interaction with the ambient medium rather than by relativistic beaming.

Morphological properties of the sources in this sample are similar to those found in the smaller CSS by Dallacasa et al. (1995).

H_0=100 km sec^{-1} Mpc^{-1}, and q_0=0.5 have been assumed throughout this paper.

Key words: galaxies: active – quasars: general – radio continuum: galaxies

Send offprint requests to: C. Stanghellini

1. Introduction

The GHz Peaked Spectrum (GPS) radio sources are extremely powerful ($L_{radio} \approx 10^{45}$ erg sec^{-1}) very compact (10 – 100 mas, 10 – 1000 parsecs) sources characterized by a simple convex spectrum which peaks near 1 GHz (O'Dea et al. 1991, O'Dea and Baum 1997, and references therein).

Recently, we have concentrated our research on a comprehensive (optical/radio) study of a complete sample of these objects selected from the catalogue of 1 Jy radio sources by Kühr et al. (1981).

The selection criteria are: a) declination $\delta > -25^o$; b) galactic latitude $|b| > 10°$; c) flux density at 5 GHz $S_{5GHz} > 1Jy$; d) observed turnover frequency between 0.4 and 6 GHz; e) spectral index $\alpha_{thin} > 0.5$ ($S_\nu \propto \nu^{-\alpha}$) in optically thin part of the spectrum. The final complete sample consists of 33 objects (Stanghellini 1992, Stanghellini et al. 1996,1997).

Radio data obtained with the Very Large Array (VLA) and the Westerbork Synthesis Radio Telescope (WSRT) at various frequencies allow a detailed study the shape of the radio spectrum and the polarization properties of the sources from the complete sample (Stanghellini et al. 1997).

Optical observations at the Nordic Optical Telescope and the Issac Newton Telescope in La Palma (Canaries Islands) and at Kitt Peak and Lick Observatory (USA) have been used to image a number of GPS radio galaxies and to find the redshifts for the sources without such information (O'Dea et al. 1990; Stanghellini et al. 1993; O'Dea et al. 1996b, 1997 in preparation).

Our results can be summarized as follows:

GPS sources tend to show a narrow convex radio spectrum with a very steep low frequency turnover suggesting the existence of either synchrotron self-absorption or external absorption (free-free or Induced Compton).

The fractional polarization with few exceptions is very low ($< 0.5\%$) at cm wavelengths implying a high degree of Faraday depolarization and/or a disordered magnetic field.

CCD imaging of GPS sources suggests that the majority of them are currently interacting.

Numerical simulations (Hernquist 1989, Barnes and Hernquist 1991) show that in interacting or merging systems a large amount of gas can be driven into the inner part (a few hundred parsecs) of a galaxy in time scales of the order of 10^8 years. The low radio polarization suggests the existence of a dense gas in the near-nuclear ISM, while the optical evidence for strong interaction and/or merging suggests that the dense near-nuclear gas was acquired in a merger.

A few GPS radio sources ($\sim 5-10\%$) were found to have associated weak, diffuse radio structure on the 10-100 kpc scale (Baum et al 1990, Stanghellini et al. 1990).

Optical and radio observations lead to the suggestion that the GPS sources are formed when the radio source interacts with an unusually dense and clumpy medium on scales typical of the Narrow Line Region (NLR) or even smaller. This could lead to 3 basically different evolutionary scenarios:

The youth scenario: Phillips and Mutel (1982) first suggested that GPS radio galaxies could be extended classical double radio sources at the very first stage of their life. This hypothesis is applied only to the GPS sources showing compact double morphology.

Recently support for this hypothesis has been provided by Fanti et al. (1995) who considered the evolution of CSS and GPS radio sources. Fanti et al. note that there is continuity in the observed properties of CSS and GPS sources (see also Fanti et al 1990; and O'Dea and Baum 1997) and they suggest that CSS sources are just a scaled up version of GPS sources (either older and/or with a less dense ambient medium), with a turnover in the radio spectrum occurring at lower frequencies. Fanti et al. (1995) suggest that for the objects with double morphology, even if the ambient environment is denser and clumpier than expected, the radio source cannot be confined, and based on the sizes and estimated expansion speeds, the inferred age of the CSS sources is of the order of 10^6 years. Similar conclusions have been reached by Readhead et al. (1996a,b).

The short lifetimes implied for GPS sources suggest that they should be very rare compared to the large scale FRI and FRII radio galaxies. Given the fraction of CSS and GPS sources in flux limited catalogues, strong luminosity evolution is required for consistency with the relative numbers - i.e., the sources must dim as they age.

Fanti et al (1995), Readhead et al (1996a,b), O'Dea and Baum (1997) argue that the radio source luminosity decreases by a factor of 10 as the size of the radio source grows from a few to hundreds of kpc.

These results lead to an evolutionary scenario where GPS/CSS radio sources evolve in intermediate power extended radio sources rather than in high power radio sources as first suggested by Phillips and Mutel (1982).

The frustration scenario: This hypothesis suggests that GPS radio sources will never become as large as the classical doubles since the dense and clumpy environment is able to confine and trap the radio emitting region on the scale of the NLR (van Breugel et al. 1994, O'Dea et al. 1991, Carvalho 1994). O'Dea et al. (1996a) studied 2 GPS radio sources with ROSAT and found they are not observed to be strong X ray emitters, implying that they are intrinsically weak in soft X-rays and/or they are highly obscured by cold material, which might be able to provide the density needed to confine the radio sources for ages comparable to those of extended radio sources. Further studies of the cold gas content of the host galaxies are needed.

The recurrent activity scenario: An alternate hypothesis has been proposed to explain the kpc scale radio emission seen around $\sim 5-10\%$ of GPS radio sources (Baum et al. 1990, Stanghellini et al. 1990). They suggest that at least this fraction of GPS radio sources have recurrent nuclear activity. The relic of the past activity is still present while the reborn radio source digs its way through the near-nuclear ISM.

The morphological properties of GHz-Peaked-Spectrum radio sources on the parsec scale may shed some light on the origin and evolution of powerful radio galaxies. In the past years many objects have been observed with the VLBI and more recently with the Very Large Baseline Array (VLBA). A number of GPS sources have been observed by the Bologna group (Dallacasa et al. 1995 and references therein), and by the Caltech-Jodrell Bank group (Taylor et al. 1996, Readhead et al. 1996a,b and references therein), because they were included in samples of CSS or flat spectrum sources.

Early evidence from VLBI observations was that GPS quasars had asymmetric or complex shapes and GPS galaxies were compact double (CD) or triple sources, i.e. objects showing two or three components of comparable flux density, separated by a few to a few tens of mas (Phillips and Mutel 1982; Hodges et al. 1984; Mutel et al. 1985; Pearson and Readhead 1984, 1988). More sensitive VLBI observations have revealed many more details like the detection of weak cores in doubles, and substructures like lobes or jets (Conway et al. 1992,1994; Dallacasa et al. 1995; Taylor et al. 1996). These new pieces of evidence made the old classification obsolete and led to the recognition of the new separate subclass of Compact Symmetric Object (CSO) (Conway et al. 1994, Wilkinson et al. 1995) consisting of sources formerly defined as double or triple.

Most of the GPS quasars and all the GPS galaxies studied so far show low variability and no superluminal motion suggesting that, in general, these objects are not significantly Doppler boosted.

We started a project to study the morphologies on the parsec scale of our complete sample. Many GPS radio sources in our complete sample did not have detailed VLBI images, and we obtained new observations to obtain this information. Here we present the results of our VLBI imaging of 9 GPS radio sources at 5 GHz.

An extensive study on the mas morphology of CSS radio sources has been done (or is near completion) mainly in Manchester, Bologna, and Dwingeloo (Spencer et al. 1989; Fanti et al. 1985; Dallacasa et al. 1995, 1997*b*). Our results extend to-

Table 1. Antennas involved in the VLBI experiment. The nominal system equivalent flux density (SEFD) in column 3 is given by the ratio between the system temperature (in K) and the antenna gain (in K/Jy).

Antenna	Diam. (m)	nominal SEFD (Jy)
Onsala (Swe)	20	990
Effelsberg (Ger)	100	44
WSRT (NL)	93	107
JBNK2 (UK)	25	344
Medicina (Ita)	32	290
Noto (Ita)	32	194
Green Bank (US)	43	130
VLBA-KP (US)	25	300
VLBA-PT (US)	25	300
VLBA-NL (US)	25	300
VLBA-BR (US)	25	300
VLBA-OV (US)	25	300
VLBA-SC (US)	25	300
VLBA-HN (US)	25	300
VLA (US)	25	330

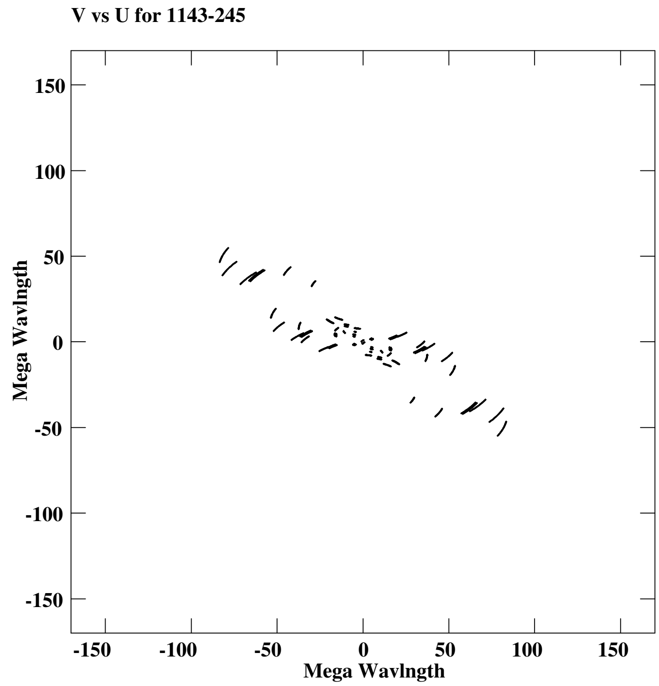

Fig. 1. UV-coverage at a declination of $-25°$

wards higher turnover frequencies the studies done on CSS radio sources.

2. Observations and data reduction

The observations were carried out in February 1993 at 4.992 GHz using a global VLBI network and the MK II recording system with 1.8 MHz bandwidth in left circular polarization (LCP). The list of antennas is given in Table 1.

Snapshots for a total of about two hours of observing time were taken for each source; however high declination objects had longer observing times than low declination sources, because of their longer mutual visibility intervals. To increase the efficiency of the observations, subnetworking restricted to EVN and VLBA (plus VLA and Green Bank) has been performed, improving the uv coverage at short to medium-length baselines. We present the typical uv coverage for 4 sources at different declinations in Fig. 1 through 4.

The data were correlated at the Caltech/JPL Block II correlator. The Astronomical Image Processing System (AIPS) developed by the National Radio Astronomy Observatory (NRAO), has been used for editing, calibration, fringe-fitting, imaging and self-calibration.

The flux density scale was calibrated using the compact radio sources 0016+731, 0235+164, and DA193, with adopted flux densities of 1.71 Jy, 3.97 Jy, and 6.95 Jy respectively as measured at Effelsberg and/or at the WSRT during the same VLBI session. The visibility function of every calibrator has been inspected, and we excluded the transatlantic baselines in the determination of the "b-factors" in order to avoid effects due to resolution. This resulted in a separate amplitude calibration of the European and American telescopes.

After the application of the *a-priori* amplitude calibration the data were fringe fitted, then we applied the standard techniques of imaging and self-calibration. Several iterations of interactive phase self-calibration were performed until we converged to an acceptable solution. Then one or more iterations of amplitude and phase self-calibration were applied.

In VLBI the performances of the antennas are not simply correlated with the system temperature (Tsys) and the antenna diameter. Other non-predictable instrumental and/or atmospheric causes may affect the data. Therefore various weighting functions have been used according to the visibility functions of each source, rather than using a single recipe for all the sources, or simply using the weights generated by AIPS.

The final images are shown in Fig. 5 through 14.

3. Results

The list of the observed radio sources with the basic information is shown in Table 2.

The parameters of the various components are shown in Table 3 and were measured on the images. Compact components, if not otherwise specified, were considered distinct if their separation was greater than the beam size. Extended emission regions have been considered distinct if well separated.

We assume a 10% formal error on the fit parameters (unless otherwise specified) based on the differences in the results obtained from various fits to the same component varying the fitting box.

Table 2. GPS sources. Columns 1 through 11 provide: (1) name, (2) and (3) B1950 coordinates, (4) optical identification, (5) optical magnitude, (6) redshift, (7) linear scale factor pc/mas [H_o=100 km s^{-1} and q_o= 0.5 have been assumed]. A value of z = 1 has been considered for one Stellar Object without redshift, and z = 0.5 for one Galaxy without redshift, assumed to be typical values for GPS quasars and radio galaxies respectively (8) maximum VLBI angular size, (9) maximum VLBI linear size, (10) flux density at 5 GHz, as measured by the VLA, (11) flux density at 5 GHz as measured from our VLBI images (12) low frequency spectral index (13) high frequency spectral index, and (14) computed turnover frequency (the values in column 10,12,13,14 are from Stanghellini 1992; Stanghellini et al. 1997). We note that high frequency variability might have affected a few sources, so the flux density measured by Stanghellini et al. (1997) could be different from the total flux density at the epoch of the observations. References for the information given here are listed in the comments for the individual sources

Source	*RA* $B1950$	*DEC* $B1950$	*id*	*m*	*z*	*scale* pc/mas	θ_{max} mas	l_{max} pc	S_{vla} Jy	S_{vlbi} Jy	α_l	α_h	ν_m GHz
0500+019	05 00 45.18	+01 58 53.8	G	21.0i	0.583	3.8	15	57	1.89	1.93	-1.64	0.60	1.8
0738+313	07 38 00.18	+31 19 02.1	Q	16.1V	0.630	3.9	9	36	3.62	2.78	-0.72	0.83	5.3
0742+103	07 42 48.47	+10 18 32.6	Q?	23R	(1)	4.3	13	(56)	3.46	3.49	-0.66	0.63	2.7
0743−006	07 43 21.05	−00 36 55.8	Q	17.5V	0.994	4.3	6	26	2.05	1.95	-0.88	0.61	5.8
1143−245	11 43 36.37	−24 30 52.9	Q	18.5V	1.95	4.1	7	30	1.40	1.38	-1.41?	0.65	2.2
1345+125	13 45 06.17	+12 32 20.3	G	15.5r	0.122	1.5	85	130	3.05	2.65	-0.67	0.50	0.4
2126−158	21 26 26.78	−15 51 50.4	Q	17.3V	3.270	3.5	6	20	1.17	1.18	-1.29	0.50	4.1
2128+048	21 28 02.61	+04 49 04.4	G	23.3r	0.99	4.3	35	150	2.02	2.02	-0.93	0.81	0.7
2210+016	22 10 05.13	+01 37 59.5	G?	22.0i	(0.5)	3.6	80	(290)	1.05	0.76	-0.61	0.83	0.5

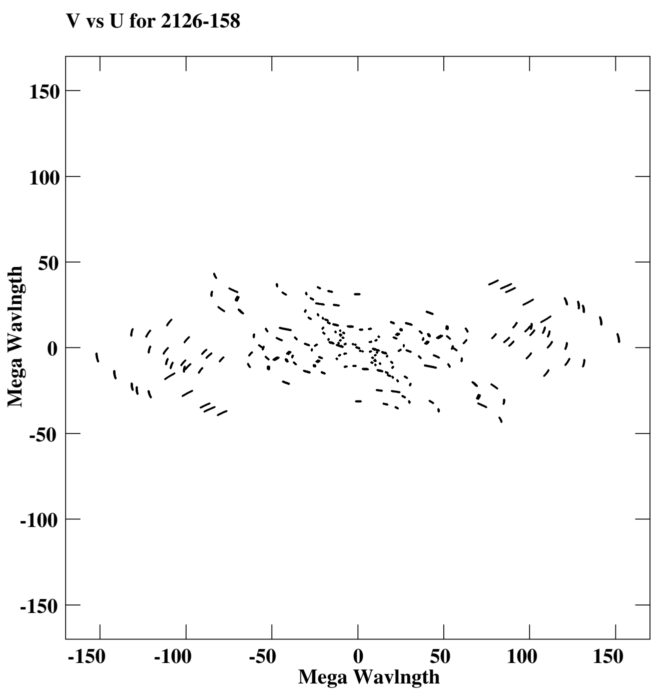

Fig. 2. UV-coverage at a declination of −16°

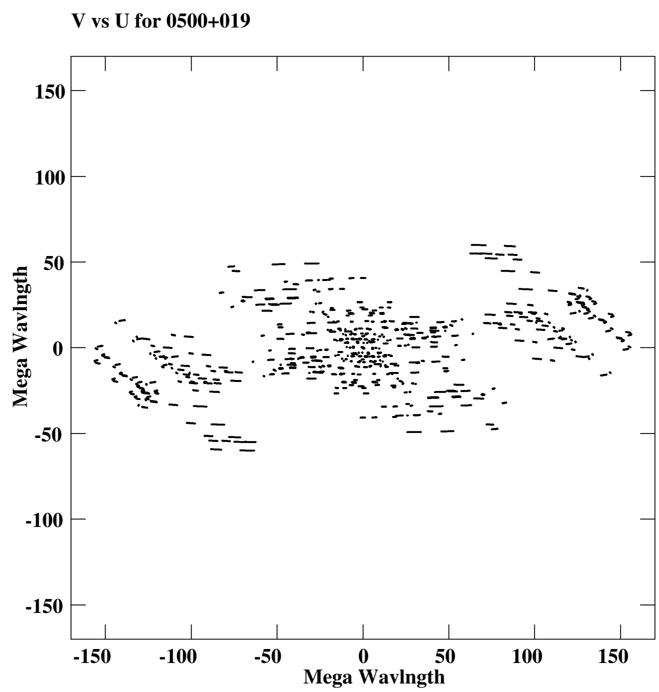

Fig. 3. UV-coverage at a declination of +2°

In Table 3 we report either the Full Width Half Maximum (FWHM) size derived from the gaussian fits on the image for slightly resolved components or the whole extension approximately measured on the image for very extended components (marked with different symbols).

The sum of the flux densities of the various components does not correspond exactly to the total flux density measured at the VLA (Table 2, Stanghellini et al. in preparation), being in any case well within the uncertainty of the measurements. All the sources but one (0738+313, see below) are pointlike at the VLA resolution, but also for 0738+313 the VLA flux density reported is referred to the main unresolved VLA component.

The equations to calculate the physical parameters with the assumption of a homogeneous spherical region radiating by incoherent synchrotron emission can be derived from Pacholczyk (1970). The minimum energy and corresponding magnetic field are given by

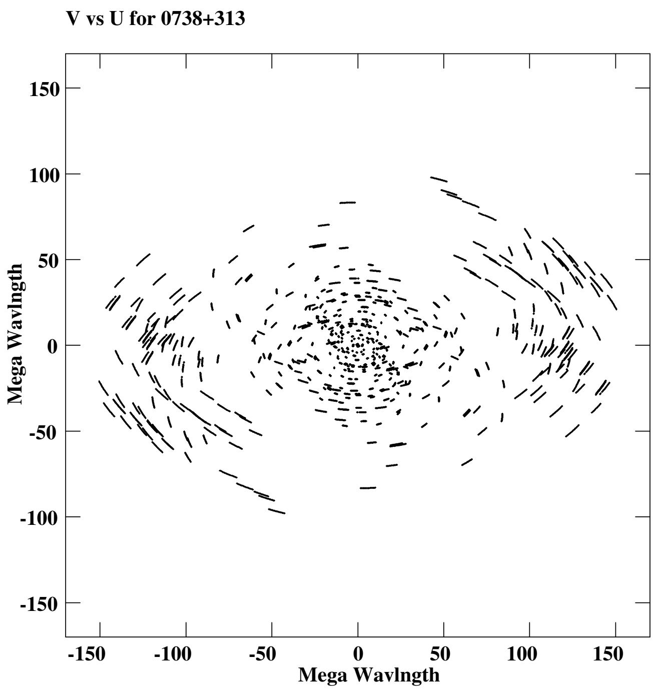

Fig. 4. UV-coverage at a declination of +31°

$$u_{min} \approx (13.06\alpha+0.294)\times 10^{-24}\phi^{\frac{3}{7}} P_{1.4}^{\frac{4}{7}} V_{kpc^3}^{-\frac{4}{7}} (1+\eta)^{\frac{4}{7}}\ erg/cm^3$$

$$H_{eq} \approx (24 \times \frac{\pi}{7} \times u_{min})^{0.5} Gauss$$

where $P_{1.4}$ is the radio luminosity in W/Hz at 1.4 GHz, ϕ is the filling factor (assumed to be 1), η the ratio protons/electrons (assumed to be 1), V_{kpc^3} is the volume in kpc assuming the size along the line of sight the same as the minor axis. The spectral index α have been assumed to be 0.75 ($S \propto \nu^{-\alpha}$).

The brightness temperature has been calculated with the formula:

$$T_b = \frac{2c^2}{\pi k \nu^2} \frac{S}{(\theta_1 \times \theta_2)^2} (1+z)$$

$$\approx 1.36 \times 10^{12} \frac{4}{\pi \nu^2} \frac{S_{Jy}}{(\theta_1 \theta_2)^2} (1+z)\ K^{\circ}$$

In the formulas above θ_1 and θ_2 have been multiplied by 1.8 if gaussian FWHM were used (Marscher 1977).

3.1. Comments on individual sources

0500+019

Fugmann and Meisenheimer (1988) found the optical counterpart of 0500+019 to be a pointlike source with a nearby extended companion, while di Serego Alighieri et al. (1994) found it slightly resolved. De Vries et al. (1995) consider the parent object a galaxy and measure a redshift of z = 0.583. Stickel et al. (1996) find an asymmetric galaxy of magnitude m_R=20.7 as the optical counterpart of the radio source and find the morphology dominated by a point source in the infrared (λ = 2.16μm). They also find in addition to the z = 0.583 redshift system, an unidentified emission line at 6543Å not seen in the spectrum previously presented by de Vries et al (1995). Stickel et al. (1996), based on the detection of the emitting line, to the pointlike VLBI morphology (Hodges and Mutel 1984), and the flux density variability at 22 GHz [Sic] from Stanghellini et al. 1990, suggest that the radio source is associated with a background quasar.

Our image (Fig. 5) resolves the structure of 0500+019 revealing an S-shaped morphology oriented in the NS direction accounting for the whole VLA flux density. The large flux density variability at 22 GHz stated by Stickel et al (1996) is probably based on a misunderstanding of the data in Stanghellini et al. (1990) where the flux densities given are referred to the wavelength, not to the frequency. At 5 GHz where many flux density measures are available the radio source is stable within the errors (Perley 1982, Kühr et al. 1981, O'Dea et al. 1990). Therefore we prefer the association of the radio source with the galaxy at z = 0.583 rather than with the background candidate quasar at an unknown redshift. The weak emission line seen at 6543Å by Stickel et al. (1996) could well be an artifact or a local fluctuation of the noise, and the existence of a background quasar requires further confirmation.

It is difficult to provide a morphological classification with an image at a single frequency, but the radio structure is symmetric and is dominated by components similar to jets and/or micro-lobes with the possible presence of a weak core. Such an S-shaped structure is commonly found among GPS radio galaxies (Taylor et al. 1996) and symmetric or quasi-symmetric structures are preferably found in galaxies rather than in quasars (Dallacasa et al. 1995). This is also evident in other sources of the small sample presented here.

0738+313

This object is a quasar with visual magnitude of m_V = 16.16 at a redshift z = 0.631 (Hewitt & Burbidge 1993). It has been detected by IRAS at 60μ with a flux density of 145±9 mJy (Heckman et al. 1994). Murphy et al. (1993) find extended low surface brightness emission around this source on the arcsecond scale. The core cannot be identified in our image (Fig 6). A ∼5 mas double structure is visible in the NS direction (components A and B), then a trail of emission leading SW for another ∼5 mas (components C and D). Only about 77% of the total flux density is accounted for in our VLBI image.

0742+103

Stickel and Kühr (1996) consider 0742+103 an empty field since they do not detect anything in their R-band CCD image with a limiting magnitude of m_R=22. However, previous observations from Fugmann et al. (1988) suggest an optical identification with a faint object at a magnitude $m_R \approx$ 23. Also de Vries

Table 3. Size and flux density of the components in the VLBI images. The columns give: (1) source name and possible classification (CSO:Compact Symmetric Object; CJ: core-jet; CX: complex), (2) component identification, (3) and (4) major and minor axes (fitted gaussian FWHM for compact components, approximate visible size for extended components), (5) and (6) linear size derived from columns 3 and 4, (7) position angle, (8) total flux density of the component, (9) intrinsic brightness temperature neglecting relativistic effects, (10) minimum energy density, (11) equipartition magnetic field. The scale factor for each source is that given in column 5, Table 2

Source and class	Comp.	θ_1 mas	θ_2 mas	l_1 pc	l_2 pc	PA	S_{5GHz} mJy	T$_b$ $10^9 K^\circ$	u$_{min}$ $10^{-6} erg/cm^3$	H$_{eq}$ $10^{-3} G$
0500+019	A	1.8	0.8	6.8	3.0	+125	800	19	250	52
CSO	B	1.5	0.5	5.7	1.9	+165	890	40	510	74
	C	2.0	0.5	7.6	1.9	+160	60	2.0	93	32
	D	1.2	1.0	4.6	3.8	+105	260	7.4	130	38
0738+313	A	1.1	0.2	4.3	0.8	+5	610	97	1470	126
CX	B	1.0	0.4	3.9	1.6	+145	2070	182	1410	124
	C	0.9	0.6	3.5	2.3	+145	90	5.9	158	41
	D$_{ext}$	3	3	11.7	11.7	-	35	0.43	19	15
0742+103	A	3.2	0.9	13.8	3.9	+175	3200	48	542	76
CX	B$_{ext}$	9	7	38.7	30.1	+120	220	0.5	17	14
0743-006	A	1.2	0.2	5.2	0.9	+50	1900	340	3910	205
CJ	B$_{ext}$	4	2	17.2	8.6	+45	40	0.71	43	22
	C	1.9	0.6	8.2	2.6	+20	5	0.19	29	18
1143-245	A	<1.3	<1.3	<5.3	<5.3	-	1100	>41	>760	>90
CJ	B	6.0	1.4	24.6	5.7	+5	240	1.8	122	36
1345+125	A	1.9	0.6	2.9	0.9	+160	440	9.3	200	47
CSO	B	3.9	1.2	5.9	1.8	+150	460	2.4	62	26
	C	5.6	1.5	8.4	2.3	+155	150	0.43	21	15
	D$_{ext}$	30	40	45	60	+30	1430	0.09	1.8	4.4
	E$_{ext}$	5	5	7.5	7.5	-	30	0.09	6.0	8.0
	F$_{ext}$	5	5	7.5	7.5	-	40	0.12	7.0	8.7
2126-158	A	<1.2	<1.2	<4.2	<4.2	-	350	>22	>1090	>109
CJ	B	2.7	0.3	9.5	1.1	+10	840	95	5540	244
2128+048	A	1.3	0.5	5.6	2.2	+180	20	1.3	97	32
CSO	B	4.2	1.3	18.1	5.6	+175	220	1.7	65	27
	C	3.2	2.9	13.8	12.5	+110	1400	6.5	88	31
	D$_{ext}$	8	4	34.4	17.2	-20	200	0.89	33	19
	E	3.2	1.6	13.8	6.9	+5	150	1.3	48	23
2210+016	A	5.0	3.5	18.0	12.6	+160	160	0.30	9.6	10
CSO	B	6.4	2.4	23.0	8.6	+70	120	0.25	11	11
	C$_{ext}$	15	8	54.0	28.8	+90	40	0.04	2.5	5.2
	D	5.1	2.9	18.4	10.4	+130	250	0.55	15	13
	E$_{ext}$	20	20	72	72	-	150	0.04	1.6	4.1

(private communication) finds a hint of fuzzy emission at m$_r$ $\sim$ 23, while de Vries et al. (1995) do not find any object brighter than magnitude 23 in their $i-$band observation.

GPS radio galaxies are generally found to be 0.5 - 1 mag brighter in the i band than in the Gunn-r or Cousin-R bands (O'Dea et al 1996b; Stanghellini et al 1993). The non detection in the i band might be explained if 0742+103 is a very faint quasar with an emission line in the R band strong enough to give a detection. Alternately, it could be a faint galaxy if either the r or i band measurements are in error.

Given the uncertainties of the measured magnitudes our identification of 0742+103 as a quasar is also very uncertain and requires confirmation. We assume a value of 1 for the redshift of this object. If the possible emission line falling in the red optical band is the broad emission line MgII 2798, very strong in many quasars, the resulting redshift is close to the assumed value. If 0742+103 is a quasar, it may be at very high redshift or may be highly obscured.

In our VLBI image (accounting for the whole flux density) a trail of weak emission (B) is detected East of the main component (A) which is resolved in NS direction (Fig. 7).

0743-006

The optical identification is a quasar of visual magnitude m_V=17.1 at a redshift z = 0.994 (Hewitt & Burbidge 1993). Tornikoski et al. (1993) find this source strongly variable at 90

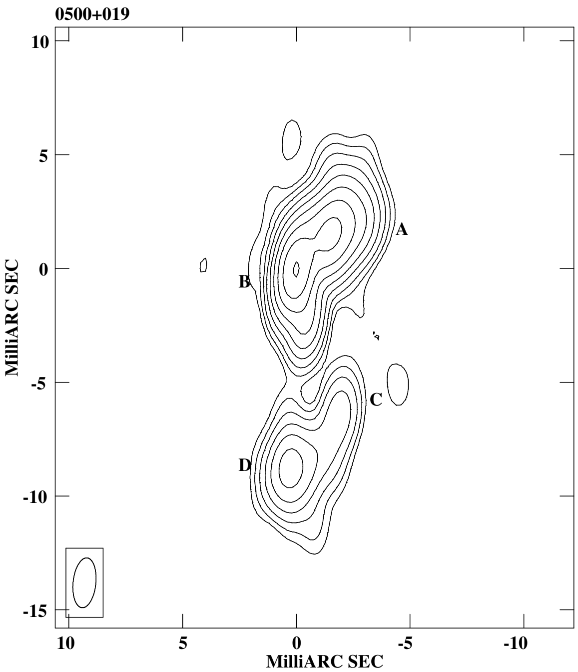

Fig. 5. 0500+019: the restoring beam is 2.2 × 1 mas in p.a. $-6°$, the rms noise on the mage is 0.8 mJy/beam, the contour levels here and in the following figures are -3, 3, 6, 12, 25, 50, 100, 200, 400, 800, 1500, 3000, 6000, 120000 times the rms noise, the peak flux density is 678 mJy/beam. The image is superresolved of a factor 1.5 in the NS direction to reveal its S-shape structure more clearly.

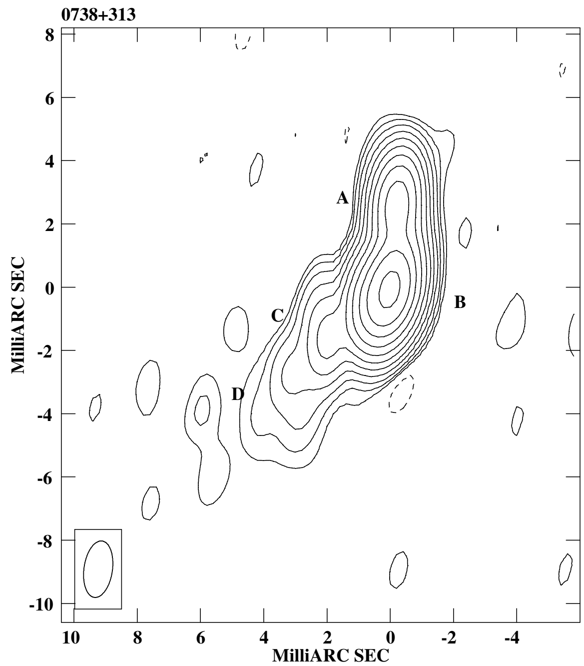

Fig. 6. 0738+313: the restoring beam is 1.8 × 0.9 mas in p.a. $-8°$, the rms noise on the mage is 0.4 mJy/beam, the peak flux density is 1546 mJy/beam.

GHz. A compact component (A) with emission extending $\sim$ 3 mas in the NE direction (B, C) makes this object a classical core-jet radio source (Fig. 8). Within the errors, the whole flux density is accounted for in the image.

1143-245

Little information is available in literature for this low declination object. It is a quasar of visual magnitude m_V=18.5 at a redshift z = 1.95 (Hewitt & Burbidge 1993). Our image shows a core-jet morphology extending in the NS direction, and accounting for the total flux density of the source (Fig. 9).

1345+125

This object at a redshift of 0.122 is one of the closest GPS radio sources known. O'Dea et al. (1996a) find an upper limit for the X ray emission on the order of $L_x < 3 \times 10^{42}$ erg s^{-1}. This upper limit suggests (1) that this object is not in an X-ray bright rich cluster, (2) the hot ISM is not enough to confine the radio source, (3) there is no cooling flow in the host galaxy, (4) the AGN is either obscured or intrinsically a weak X-ray emitter. Stanghellini et al. (1993) find that the galaxy (m_r =15.5) hosting the radio source is the dominant galaxy of a poor cluster, and has a double nucleus indicating that it is in process of merging (cf. Hutchings et al 1988; Baum et al. 1988; Smith & Heckman 1989). 1345+125 is also a ultraluminous $IRAS$ galaxy with a flux density at 60μ and 100μ of 2.01Jy and 2.14Jy respectively, even if its infrared flux density is well below that predicted by the IRAS-radio correlation (Crawford et al. 1996). Our image (Fig. 10) shows a well defined structure. From a bright knot (which we tentatively identify as the core) in the northernmost part of the source (A) a jet leads SE, then bends and expands into a diffuse lobe (D). The jet is disrupted at $\sim$30 mas from the core as already shown by Shaw et al. (1992), who interpreted it as an artifact in their image. Some knots (B, C) are present in the jet. Weak emission (E) is also detected North of the core candidate, and there is an additional weak component (F) $\sim$20 mas NW. Spectral information is necessary to unambiguously locate the core. Only about 87% of the total flux density is accounted for in our VLBI image, suggesting the presence of additional emission resolved out by the present observation.

2126-158

This is a distant quasar (z=3.266) of visual magnitude m_V = 17.3 (Hewitt & Burbidge 1993). This object has been extensively studied because of the presence of a crowded Lyman-alpha forest in its optical spectrum (e.g. Giallongo et al. 1993). It has been detected by the Einstein X-ray satellite (Wilkes et al. 1992).

The VLBI image (Fig. 11) shows a compact component. The observing beam is elongated in the NS direction and has apparently blended the NS structure of the source. A fit on the image reveals the presence of 2 components at least (Fig. 12), the northern (A) still unresolved, while the southern (B) is resolved. We show also an image superresolved by a factor of 2 along

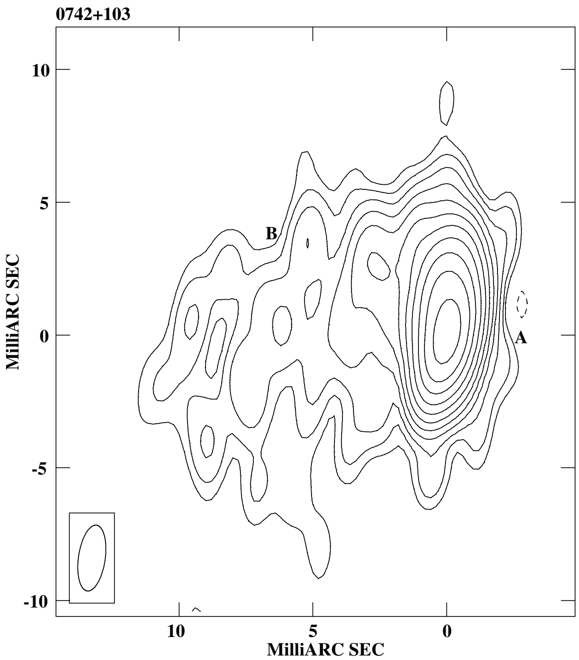

Fig. 7. 0742+103: the restoring beam is 2.5×1.0 mas in p.a. $-8°$, the rms noise on the mage is 0.4 mJy/beam, the peak flux density is 1872 mJy/beam.

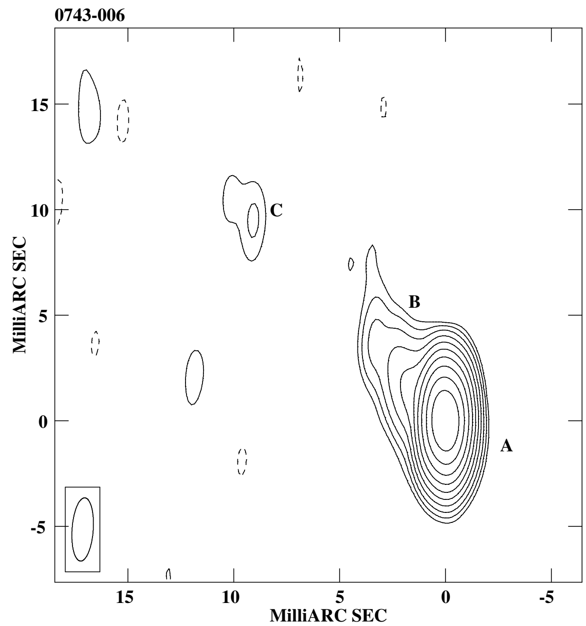

Fig. 8. 0743-006: the restoring beam is 3×1.0 mas in p.a. $-4°$, the rms noise on the mage is 0.5 mJy/beam, the peak flux density is 1354 mJy/beam.

the major axis (obtained convolving the clean components with a smaller restoring beam) in order to highlight this extended southern component, which suggests that the morphology is core-jet. The fit on the superresolved image gives the same sizes derived before, although the flux density distribution is different with about 100 mJy moved from the extended to the compact component. Due to the beam elongation along the source axis, the accuracy of the brightness distribution is not as high as in other cases. A weak $\sim$ 3 mJy component (not shown in table 3) is tentatively found on the opposite side of the core candidate (A).

2128+048

This radio source is found associated to a very red galaxy (magnitudes m_r = 23.3, m_i = 21.85) by Biretta et al. (1985). The redshift is 0.990 (Stickel et al. 1994). Early VLBI observations at 18 cm were made by Hodges et al. (1984) who found the radio source consisting of 2 resolved components separated by 29 mas along PA 169°. In our image (Fig. 13) the radio emission extends for $\sim$ 40 mas in NW-SE direction and resembles the scaled down structure of a Classical Double. At the edges there are 2 hot-spots/lobes (C, E); there is a central weak component (A) that we assume is the core, and a jet (B) connecting the core to the northern lobe. At the northern edge the radio emission seems to sharply bend to the west (D).

2210+016

This object was identified with an unresolved object of magnitude m = 21.7 by Fugmann et al. (1988; see also and Stickel and Kühr 1996). However, de Vries et al. (1995) found a counterpart with magnitude m_i=22.0, which they suggest is a galaxy. We tentatively use this last classification.

The transatlantic baselines completely resolve out the source. Even the continental baselines miss a large fraction of the flux density. Only about 75% of the total flux density is accounted for in the image (Fig. 14), which shows a $\sim$ 50 mas structure elongated in EW direction with blobs and bridges between them. A weak hint of emission (E) is also detected $\sim$30 mas SW of the eastern blob (A), confirmed by an image at 13 cm by Dallacasa et al. (1997a).

4. Discussion

The classification of the sources was based on their morphologies as core-jet (CJ), complex (CX), and compact symmetric objects (CSO). We classify as CSO candidate the radio sources showing the presence of jets and/or lobes and/or hot-spots on the opposite sides of an hypothetical center of activity. If a flat spectrum core component is shown to exist, the classification as CSO becomes certain. Images at another frequency are needed to determine the location of the cores.

We find 4 new CSO candidates. 0500+019 shows an S-shaped morphology (commonly found among GPS radio galaxies, Taylor et al. 1996) and so does 2210+016. Also 1345+125 might be classified in the same class due to a large diffuse lobe in the southern end and a small extended feature on the northern

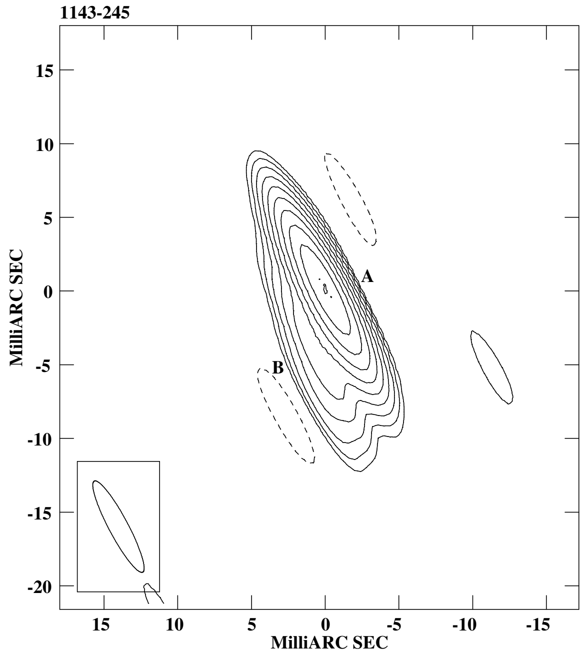

Fig. 9. 1143-245: the restoring beam is 7 × 1.3 mas in p.a. +28°, the rms noise on the mage is 0.7 mJy/beam, the peak flux density is 1089 mJy/beam.

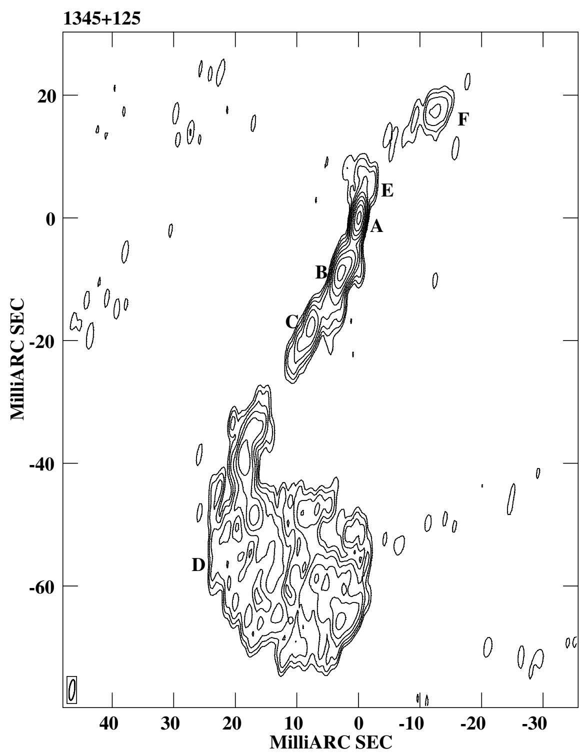

Fig. 10. 1345+125: the restoring beam is 3.4 × 0.9 mas in p.a. $-7°$, the rms noise on the mage is 0.3 mJy/beam, the peak flux density is 305 mJy/beam.

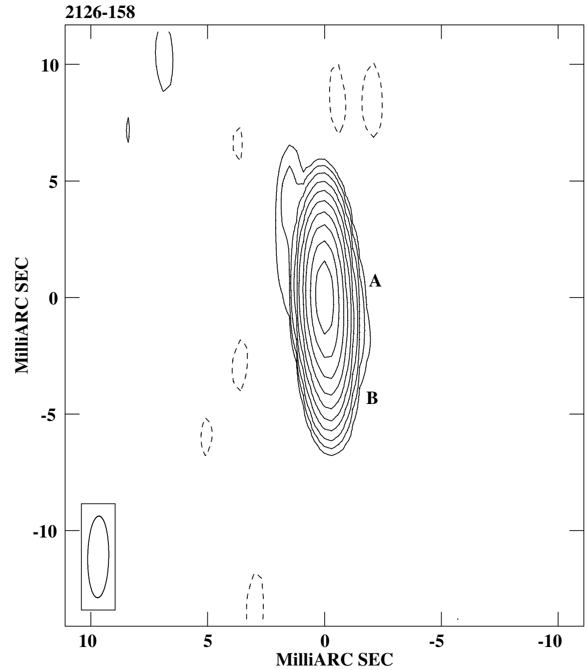

Fig. 11. 2126-158: the restoring beam is 3.5×0.9 mas in p.a. $-1°$, the rms noise on the image is 0.4 mJy/beam, the peak flux density is 922 mJy/beam.

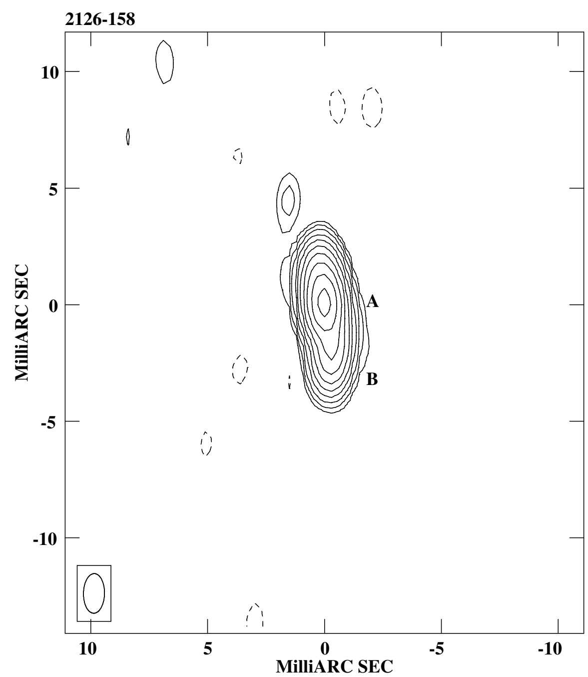

Fig. 12. 2126-158: the restoring beam is 1.7 × 0.9 mas in p.a. $-1°$, superresolved of a factor $\sim$ 2 along the major axis, the rms noise on the mage is 0.4 mJy/beam, the peak flux density is 779 mJy/beam.

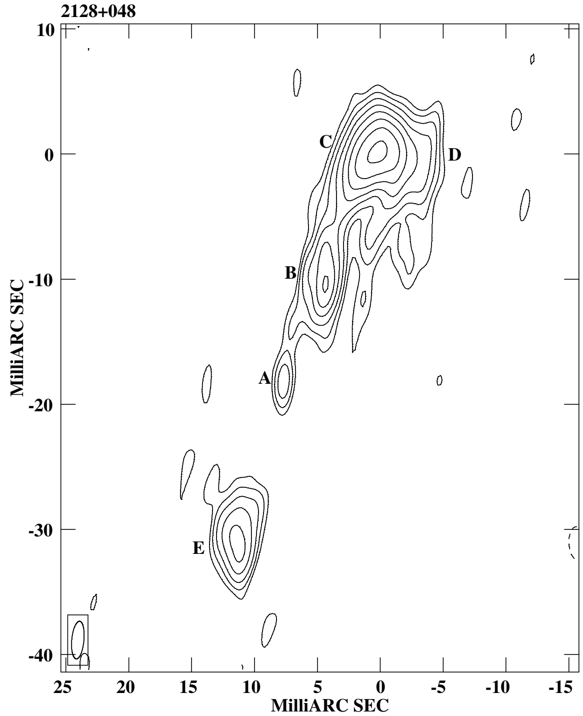

Fig. 13. 2128+048: the restoring beam is 3.0 × 1.0 mas in p.a. −5°, the rms noise on the mage is 0.8 mJy/beam, the peak flux density is 382 mJy/beam.

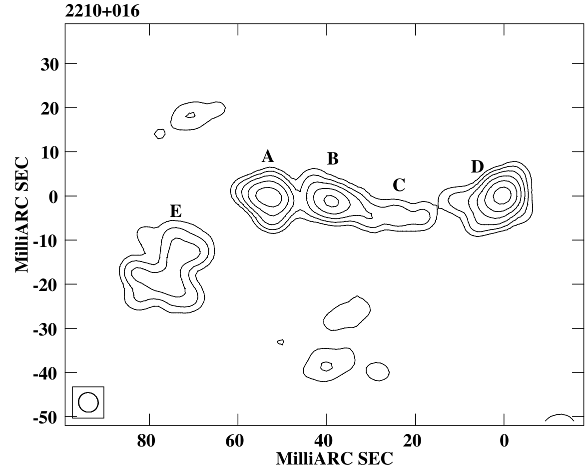

Fig. 14. 2210+016: the restoring beam is 4.5 × 4.4 mas in p.a. +43°, the rms noise on the mage is 0.8 mJy/beam, the peak flux density is 145 mJy/beam.

edge. The candidate core is the bright unresolved component at the peak position. 2128+048 shows the better defined CSO morphology with a straight structure in the NS direction. The 5 GPS quasars observed here have a core-jet or complex structure.

The projected linear sizes of the quasars are smaller than those of the galaxies: in fact they are in general smaller than 100 pc, while the galaxies have a range of sizes extending up to hundreds of parsecs (Table 1). If we consider the seven objects with measured redshift, the average linear size of the three galaxies is about four times larger than the average size of the four quasars. Assuming that all the objects belong to the same population and the galaxies are in the plane of the sky, a 1 to 4 ratio in linear size corresponds to an angle of 15° between the radio axis and the line of sight for an "average" GPS quasar.

The high flux density ratio between the two opposite sizes in the CSO candidates is consistent with relativistic Doppler boosting or interaction with the ambient medium. As noted by Readhead et al. (1996a,b), who report several cases where a large brightness ratio of the two sides does not imply a strong core, if the difference in brightness were due to relativistic beaming we would expect a strong core, unless the jets are strongly bent. The four radio galaxies presented here do not have a dominant core although unambiguous identification of the cores is needed to confirm their morphology, as previously mentioned. The presence of beaming might be expected to be accompanied by strong variability. However, strong variability is not seen in our 4 radio galaxies (Stanghellini et al. 1997).

Our conclusion is that the difference in brightness between the two sides of emission in our candidate CSO are more likely due to interaction with an inhomogeneous ambient medium rather than by beaming. Sanghera et al. (1995) reach the same conclusion on a sample of CSS radio sources.

The properties which are of great interest for the unified scheme models are the arm length ratio, the ratio of the flux densities of the two sides (or limits in the one-sided objects), misalignment angles. However a reliable study of these properties can be done only for the sources where the core has been previously identified. We will present a discussion of these parameters in a following paper based on 15 GHz data that will allow to unambiguously locate the core. Several objects of our complete sample have been observed by other authors in the framework of CSS or CSO studies (i.e., Dallacasa et al. 1995, 1997*b*; Taylor et al. 1996; Readhead et al. 1996a,b) then with the availability of the 15 GHz data it will also be possible to discuss the morphology of all or almost all the radio sources of the complete sample, with a higher statistical relevancy. Another sample of 52 GPS radio sources at a lower flux density has been selected and is being studied (Snellen et al. 1996).

The completion of these studies will shed some light on the nature and evolution of this still enigmatic class of objects.

5. Summary

We have presented Global VLBI images at 5 GHz of 9 powerful radio sources belonging to a complete flux limited sample of GPS radio sources (Stanghellini 1992, Stanghellini et al. 1996,1997).

We have shown that the GPS radio sources presented here exhibit a core-jet or complex morphology with a total extent below 100 pc in the quasars and are possibly Compact Symmetric Objects (CSO) with angular sizes reaching hundreds pc in the galaxies.

GPS radio galaxies and GPS quasars have different linear sizes and morphologies, and are possibly different classes of objects. Some of the GPS quasars may appear smaller because they are shortened by projection.

There is some evidence to be investigated further that the asymmetry is intrinsic to the radio source and it is caused by interaction with the ambient medium in GPS radio galaxies.

Observations at another frequency at least are needed to locate the core, confirm the classification and determine the spectral index of the different components.

We have recently observed the same sources at 15 GHz. These new data will allow us to study this class of radio sources in much greater detail.

Acknowledgements. C.S. wishes to thank the STScI for providing support from the Collaborative Visitors Fund for his visit. The WSRT is operated by the Netherlands Foundation for Research in Astronomy with the financial support of the Netherlands Organization for Scientific Research (NWO). The NRAO is a facility of the National Science Foundation operated under cooperative agreement by Associated Universities, Inc.

References

Barnes J. E., Hernquist L. E. 1991, AJ 370, L65
Baum S.A., O'Dea C.P., Murphy D.W., de Bruyn A.G., 1990, A&A, 232, 19
Baum, S. A., Heckman, T., Bridle, A., van Breugel, W., & Miley, G., 1988, ApJS, 68, 643
Biretta J.A., Schneider D.P., Gunn J.E. 1985, AJ 90, 2508
van Breugel W.J.M., Miley G.K., Heckman T.A. 1984, AJ 89, 5
Carvalho J.C. 1994, A&A 292, 392
Conway J.E., Pearson T.J., Readhead A.C.S., Unwin S.C., Xu W., Mutel R.L., 1992, ApJ, 396, 62
Conway J.E., Myers S.T., Pearson T.J., Readhead A.C.S., Unwin S.C., Xu W., 1994, ApJ, 425, 568
Crawford T., Marr J., Partridge B., Strauss M.A., 1996, ApJ 460, 225
Dallacasa D., Fanti C., Fanti R., Schilizzi R.T., Spencer R.E., 1995, A&A 295, 27
Dallacasa D., Bondi M., Alef W., Mantovani F. 1997*a*, A&AS, submitted
Dallacasa D., Fanti C., Fanti R., Schilizzi R.T., Spencer R.E., Stanghellini C. 1997*b*, A&A in preparation
Fanti C., Fanti R., Parma P., Schilizzi R. T., and van Breugel W. J. M., 1985, A&A 143, 292
Fanti C., Fanti R., Dallacasa D., Schilizzi R. T., Spencer R. E., Stanghellini C. 1995, A&A 302, 317
Fugmann W., Meisenheimer K., 1988, A&AS 76, 145
Fugmann W., Meisenheimer K., Röser H.-J. 1988, A&AS 75, 173
Giallongo E., Cristiani S., Fontana A., Trevese D. 1993, ApJ 416, 137
Gopal–Krishna, Patnaik A. R., and Steppe H. 1983, A&A 123, 107
Heckmann T.M., O'Dea C.P., Baum S.A., Laurikainen E. 1994, ApJ 428, 65
Hernquist L. E., 1989, Nature 340, 687.
Hewitt A., Burbidge G., 1993, ApJS 87, 451
Hodges M.W., Mutel R.L., Phillips R.B. 1984 AJ 89, 1327
Hutchings, J. B., Johnson, I., & Pyke, R., 1988, ApJS, 66, 361
Kühr H., Witzel A., Pauliny-Toth I.I.K., Nauber U. 1981, A&AS 45, 367
Marscher A.P. 1977, ApJ, 216, 244
Murphy D.W., Browne I.W.A., Perley R.A. 1993, MNRAS 264, 298
Mutel R.L., Hodges M.W., Phillips R.B. 1985, ApJ 290, 86
O'Dea C. P., Baum S.A. 1997, AJ, 113, 148
O'Dea C. P., Baum S. A., Stanghellini C., Morris G. B., Patnaik A., Gopal–Krishna 1990, A&AS 84, 549
O'Dea C. P., Baum S.A, Morris G.B. 1990, A&AS 82, 261
O'Dea C.P., Baum S.A., Stanghellini C. 1991, AJ 380, 66
O'Dea C.P., Worral D.M., Baum S.A., Stanghellini C. 1996a, AJ 111, 92
O'Dea C.P., Stanghellini C., Baum S.A., Charlot S. 1996b, ApJ 470, 806
Pacholczyk A.G., 1970, in Radio Astrophysics, Freeman & C., S. Francisco
Perley R.A. 1982, AJ 87, 859
Pearson T. J., Readhead A. C. S. 1984, in "VLBI and Compact Radio Sources", IAU Symposium No. 110, R. Fanti, K. Kellermann, and G. Setti eds., Reidel, Dordrecht, p. 15
Pearson T. J., Readhead A. C. S. 1988, AJ 328, 114
Phillips R. B., Mutel R. L. 1982, A&A 106, 21
Readhead A.C.S., Taylor G.B., Xu W., Pearson T.J., Wilkinson P.N., Polatidis A.G. 1996a, ApJ, 460, 612
Readhead A.C.S., Taylor G.B., Pearson T.J., Wilkinson P.N. 1996b, ApJ, 460, 634
Sanghera H.S., Saikia D.J., Ludke E., Spencer R.E., Foulsham P.A., Akujor C.E., Tzioumis A.K. 1995, A&A, 295, 629
Smith, E. P., & Heckman, T. M., 1989, ApJ, 341, 658
di Serego Alighieri S., Danziger I.J., Morganti R., Tadhunter C.N. 1994, MNRAS 269, 998
Spencer R. E., McDowell J. C., Charlesworth M., Fanti C., Parma P., Peacock J. A. 1989, MNRAS 240, 657
Shaw M.A., Tzioumis A.K., Pedlar A. 1992, MNRAS 256, 6P
Stanghellini C. 1992, PhD thesis, University of Bologna
Stanghellini C., Baum S.A., O'Dea C.P., Morris G.B. 1990, A&A 233, 379
Stanghellini C., O'Dea C.P., Baum S.A., Laurikainen E. 1993, ApJS 88, 1
Stanghellini C., Dallacasa, O'Dea C.P., Baum S.A., Fanti R., Fanti C. 1996, in proceedings of the workshop in GPS/CSS radio sources held in Leiden NL 28 September - 1 October 1996, in press
Stanghellini C., O'Dea C.P., Baum S.A., Fanti R., Fanti C. 1997, A&A in preparation
Stickel M., Kühr H. 1996, A&AS 115, 11
Stickel M., Rieke M.J., Rieke G.H., Kühr H., 1996, A&A 306, 49
Stickel M., Meisemheimer K., Kühr H. 1994, A&AS 105, 211
de Vries W.H., Barthel P.D., and Hes R. 1995, A&AS 114, 259
Taylor G.B., Readhead A.C.S., Pearson T.J. 1996, ApJ 463, 95
Tornikoski M., Valtaoja E., Teräsranta H., Lainela M., Bramwell D., Botti L.C.L. 1993, AJ 105, 1680
Wilkes B.J., Tananbaum H., Worrall D.M., Avni Y., Oey M.S., Flanagan J. 1994 ApJS 92, 53
Wilkinson P.N., Polatidis A.G., Readhead A.C.S., Xu W., Pearson T.J. 1995, ApJ, 432, L87

This article was processed by the author using Springer-Verlag LaTeX A&A style file *L-AA* version 3.